

# Single-Shot ADC Imaging for fMRI

A. W. Song<sup>1</sup>, H. Guo<sup>1</sup>, and T-K. Truong<sup>1</sup>

<sup>1</sup>Brain Imaging and Analysis Center, Duke University, Durham, North Carolina, United States

## Introduction

Contrast mechanisms based on changes of the apparent diffusion coefficient (ADC) can be sensitive to cerebral blood flow changes<sup>1</sup> during brain activation<sup>2</sup>. However, current ADC imaging techniques inherently have a low temporal resolution due to the requirement of multiple acquisitions with different b factors, as well as potential confounds from cross-talks between the deoxyhemoglobin-induced background gradients and the externally applied diffusion-weighting gradients. To address these two limitations, we propose a new single-shot pulse sequence that sequentially acquires one gradient-echo and two diffusion-weighted spin-echo images, using numerically optimized diffusion-weighting waveforms to null the cross-terms with the background gradients and thus fully isolate the effect of diffusion-weighting from that of oxygenation level changes. The experimental results showed that this new single-shot method could acquire ADC maps with sufficient signal-to-noise ratio (SNR), establishing its practical utility in fMRI to complement the blood oxygenation level-dependent (BOLD) technique and allow differential sensitivity for different vasculatures to better localize neural activity originating from the small vessels.

## Methods

A new pulse sequence was implemented that sequentially acquires a gradient-echo and two spin-echoes with different degrees of diffusion-weighting ( $b_1$  and  $b_2$ ). The gradient-echo image was acquired immediately after the excitation and should experience minimal transverse relaxation, providing an approximation of the proton density. In practice, however, it was found that a significant amount of  $T_2^*$ -weighting still existed in the gradient-echo image, even when a minimum  $TE_0$  (4 ms) was used. To correct for this  $T_2^*$ -weighting, the acquisition windows of the two subsequent spin-echoes were offset by the same amount of time  $TE_0$ .

It is generally accepted that the BOLD background gradients can be approximated to be linear for small spatial segments and constant during the brief period of signal acquisition, especially around large vessels. In this case, conventional diffusion-weighting gradients such as a simple bipolar gradient could have significant cross-terms with these background gradients<sup>3,4</sup>. As such, we employed numerically optimized diffusion-weighting gradients which had zero cross-terms with the background gradients, herein referred to as the independent gradients (IG), as opposed to the dependent gradients (DG) using bipolar waveforms. The IG waveforms were designed by nulling the cross-terms between the applied gradients and the background gradient such that  $\int_0^t k \cdot k_b dt' = 0$ , where  $k$  and  $k_b$  are their k-space trajectories respectively.

Without the cross-terms, the exponential signal attenuation due to the background gradient and the diffusion-weighting gradients can be separated. As a result, the signals of the two spin-echoes can be expressed as:  $S_1 = M_0 e^{-TE_0/T_2^*} e^{-TE_1/T_2} e^{-b_1 D}$  and  $S_2 = M_0 e^{-TE_0/T_2^*} e^{-TE_2/T_2} e^{-b_2 D} e^{-2b_0 D}$ , where  $M_0$  is the original magnetization,  $D$  is the ADC for any given voxel, and  $b_0$  is the b factor from the BOLD background gradient seen by the first spin-echo;  $2b_0$  is then the b factor seen by the second spin-echo since  $TE_2$  was set equal to  $2TE_1$  to simplify the algebra. As such, both the  $T_2$  effect and the BOLD background b factor can be removed, resulting in:

$D = (2 \ln S_1 - \ln S_2 - \ln S_0 - (TE_2 - 2TE_1))/(b_2 - b_1) = (2 \ln S_1 - \ln S_2 - \ln S_0)/(b_2 - b_1)$ , where  $b_2 \neq b_1$ . Here  $S_0 = M_0 e^{-TE_0/T_2^*}$  is the signal intensity of the gradient-echo. To simplify the sequence design, diffusion-weighting was turned on only for the second spin-echo (i.e.,  $b_1$  was 0 s/mm<sup>2</sup> and  $b_2$  was 146 s/mm<sup>2</sup>).

A visual activation paradigm based on flashing and rotating checkerboards was used. Subjects were instructed to passively fixate on a crosshair in the center of the screen at all times. A FOV of 24 cm and a matrix size of 64 × 64 were used for all functional images. A minimum  $TE_0$  of 4 ms was used, along with  $TE_1$  and  $TE_2$  of 61 ms and 122 ms, within a TR of 2 s. Four axial slices (5 mm thickness) were acquired above and below the Calcarine fissure. 70 sets of ADC maps were acquired for each run to form a dynamic ADC time course. Four runs were acquired for each diffusion-weighting scheme (IG or DG) to ensure sufficient SNR. Six healthy volunteers were studied on a 3 T MRI scanner (GE Healthcare, Milwaukee, WI).

## Results and Discussion

A gradient-echo and two subsequent spin-echo images were acquired using our new single-shot sequence on a doped water phantom (Fig. 1a). Without diffusion-weighting gradients, the bulk of the voxels should satisfy:  $2 \ln S_1 - \ln S_2 - \ln S_0 = 0$ , which is confirmed in Fig. 1b. After turning on the IG diffusion-weighting gradients, the same sequence was used in human experiments. For comparison, ADC activation maps using the DG waveforms were also acquired. The same statistical tests based on the general linear model were performed on these two time courses to obtain activation maps.

Significant activations were found in the gradient-echo BOLD, spin-echo BOLD, and ADC activation maps. However, the gradient-echo and second spin-echo BOLD activation maps showed less activation, due to the short TE or the excessively long TE, respectively. As expected, noticeable spatial discrepancies were also seen between the IG-ADC and DG-ADC activations (Fig. 2a). In particular, the DG-ADC activation map shows a significant influence by the large veins, as evidenced by the large activation immediately adjacent to the sagittal sinus. To combine results across all subjects, a composite histogram was constructed showing all activated pixels of equal number using the IG- and DG-ADC acquisitions across all subjects as a function of the distance to the sagittal sinus (Fig. 2b). The spatial profiles of the activated pixels under these two conditions clearly demonstrate a shift (~5 mm) away from the large vessels for the IG-ADC activation. This finding is consistent with the observation that the IG-ADC activation map shows much reduced contaminations from the large vein BOLD gradients. The two activation maps were otherwise comparable and showed significant overlap.

## Conclusion

Our results demonstrate that a new single-shot technique can be used to acquire images with sufficient SNR to determine an ADC map in a single excitation, leading to a significant increase in temporal resolution. In addition, the ADC maps obtained using this sequence are independent from the  $T_2$  effect and the BOLD background gradients, resulting in a significant improvement in accuracy. These advantages can help better model the dynamic ADC changes induced by brain activation temporally and spatially, and may provide differentiating sensitivity to the small vessels from the large vessels to achieve better functional localization of the neuronal activities.

## References and Acknowledgments

1. Le Bihan D *et al.* Radiology 1986;161(2):401-407. 2. Song AW *et al.* Neuroimage 2002;17(2):742-750. 3. Zhong J *et al.* Magn Reson Med 1998;40(4):526-536. 4. Does MD *et al.* Magn Reson Med 1999;41(2):236-240. This work was supported by grants from the National Institutes of Health (NS 41328 and NS 50329).

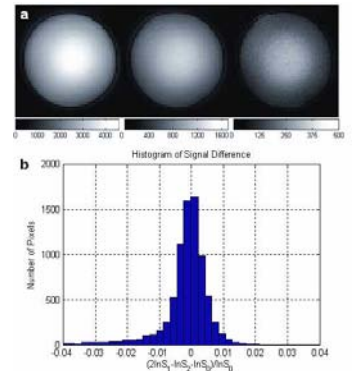


Fig. 1 a) Gradient-echo and two spin-echo images of a phantom. b) Voxel histogram of quantity  $(2 \ln S_1 - \ln S_2 - \ln S_0) / \ln S_0$ .

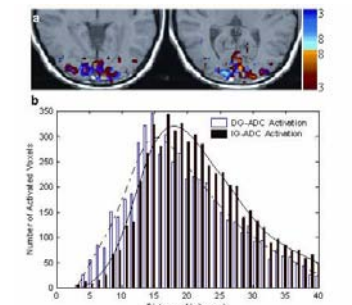


Fig. 2 a) ADC activation maps using IG (red) and DG (blue). b) Histogram of all activated voxels as a function of the distance to the sagittal sinus.